1626 *J. Phys. Chem.* **1991,** *95,* 1626-1635

High-Temperature Oxidation Mechanisms of *m*- and *p*-Xylene

J. L. Emdee, K. Brezinsky,* and I. Glassman

Mechanical and Aerospace Engineering Department, Princeton University, Princeton, New Jersey 08544-5263

(Received: June 7, 1990; In Final Form: September 11, 1990)

Mechanisms for the oxidation of *m*- and *p*-xylene were developed with the aid of atmospheric flow reactor tests at temperatures ranging from 1093 to 1199 K and equivalence ratios from 0.47 to 1.7. The experimental data suggested that *m*-xylene is oxidized by sequential oxidation and removal of the methyl side chains while *p*-xylene reacts through simultaneous, as well as sequential, oxidation of the side chains. The formation of *p*-xylylene (3,6-bis(methylene)-1,4-cyclohexadiene), postulated to occur during the oxidation of *p*-xylene, opens up the simultaneous oxidation route and leads to the formation of *p*-phthalaldehyde. The formation of *m*-xylylene during the oxidation of *m*-xylene was determined to be unfavorable. In order to better understand specific steps of the mechanisms, the oxidation of *p*-tolualdehyde and the pyrolysis of *p*-methylanisole were also studied. *p*-Tolualdehyde tests were used to show that the aldehydic side chain is consumed quicker than the methyl side chain. Because *p*-methylanisole decays quickly to methyl and *p*-methylphenoxy radical, it was used to determine the fate of methylphenoxy radical formed during the xylene tests. The results indicated that methylcyclopentadienyl and CO are formed from the methylphenoxy and that methylcyclopentadienyl rearranges quickly to benzene and hydrogen atom.

Introduction

The mechanism of the high-temperature oxidation of benzene has been studied previously in this laboratory[1,2] as well as the mechanism of toluene oxidation[3] and that of other singly alkylated aromatics such as ethylbenzene.[4] The present study of *m*-xylene (1,3-dimethylbenzene or 1,3-$CH_3C_6H_4CH_3$) and *p*-xylene (1,4-dimethylbenzene or 1,4-$CH_3C_6H_4CH_3$) was undertaken to explore the effect of multiple side chains on the oxidation of aromatic hydrocarbons. Chemistry is revealed that is both similar to and different than that of toluene.

Previous studies[5,6] of xylene oxidation chemistry have concentrated on temperature regimes of less than 1000 K where organic peroxides can play a large role in the oxidation mechanisms. In 1960, Wright[5] studied the xylenes in a static reactor at 683-823 K by following the pressure rise in the reactor. Without product distributions a mechanism was not proposed. In 1968, Barnard and Sankey[6] proposed a reaction mechanism that applied to both the meta and para isomer based on products from a static reactor at 733-785 K. These latter investigators suggested that formaldehyde was the important degenerate branching intermediate based on the relationship between formaldehyde concentration and the rate of reaction. Their mechanism, involving formaldehyde, included the formation of an organic peroxy radical and subsequent oxidation of that radical:

$$CH_3C_6H_4CH_3 + O_2 \rightarrow CH_3C_6H_4\dot{C}H_2 + HO_2$$

$$CH_3C_6H_4\dot{C}H_2 + O_2 \rightarrow CH_3C_6H_4CH_2OO^{\bullet}$$

$$CH_3C_6H_4CH_2OO^{\bullet} + O_2 \rightarrow \alpha HCHO + OH + \text{products} \quad (\alpha < 1)$$

Using equilibrium arguments, Benson[7] showed that benzylperoxy ($C_6H_4CH_2OO^{\bullet}$) decomposes to benzyl and oxygen molecule very quickly as the temperature increases beyond 500 K due to the stability of the benzyl radical. Benson's calculations are supported by recent rate data for oxygen molecule reacting with benzyl.[8,9] On the basis of similar arguments, it can be shown that methylbenzylperoxy is expected to do the same. Therefore, the mechanisms proposed previously for the oxidation of the xylenes will certainly not be valid as the temperature increases beyond 1000 K.

TABLE I: Experimental Conditions for the Flow Reactor Tests[a]

	mole fraction × 10^6				
fuel	fuel (±10%)	oxygen (±5%)	Φ^c	T_0, K	T_{final}, K
p-xylene	1660	36 800	0.47	1093	1098
p-xylene	1530	29 700	0.54	1157	1184
p-xylene	1420	16 800	0.89	1155	1161
p-xylene	1520	10 500	1.5	1155	1161
p-xylene	1420	25 600	0.58	1199	1358
m-xylene	1600	28 700	0.59	1161	1172
m-xylene	1580	16 800	1.0	1155	1161
m-xylene	1610	10 200	1.7	1158	1161
p-tolualdehyde	860	7 500	1.1	1152	1163
p-methylanisole	970	<200[b]		1043	1043

[a] The balance of the gas flow was nitrogen. [b] The *p*-methylanisole test was a pyrolysis; this is the mole fraction of oxygen in the flow reactor without added oxygen. [c] $\Phi \equiv [\text{fuel}]/[O_2]:[\text{fuel}]/O_2]_{\text{stoich}}$.

To develop a high-temperature oxidation mechanism for the xylenes, rich, lean, and stoichiometric mixtures of *m*- and *p*-xylenes were reacted in a flow reactor at temperatures from about 1100 to 1200 K and 1 atm of pressure. To aid in the development of the mechanisms, the oxidation of *p*-tolualdehyde (*p*-$CH_3C_6H_4CHO$) and the pyrolysis of *p*-methylanisole (*p*-$CH_3C_6H_4OCH_3$) were also studied in the flow reactor. The oxidation of *o*-xylene, found to be unique relative to the other isomers, was also studied and is the subject of another paper.[10]

Experimental Section

The flow reactor used during this study has been described extensively in the literature,[2-4] so only a brief description will be presented here. Hot nitrogen supplied by a plasma torch was passed through a stainless steel tube and mixed with a small amount of oxygen before entering a quartz diffuser section. At the 2.5-cm throat of the diffuser, fuel vapor from an evaporator

---

(1) Venkat, C.; Brezinsky, K.; Glassman, I. In *Proceedings of the 19th Symposium (International) on Combustion*; The Combustion Institute: Pittsburgh, 1983; p 143.

(2) Brezinsky, K. *Prog. Energy Combust. Sci.* **1986,** *12,* 1.

(3) Brezinsky, K.; Litzinger, T. A.; Glassman, I. *Int. J. Chem. Kinet.* **1984,** *16,* 1053.

(4) Litzinger, T. A.; Brezinsky, K.; Glassman, I. *Combust. Flame* **1986,** *63,* 251.

(5) Wright, F. J. *J. Phys. Chem.* **1960,** *64,* 1944.

(6) Barnard, J. A.; Sankey, B. M. *Combust. Flame* **1968,** *12,* 345.

(7) Benson, S. W. *J. Am. Chem. Soc.* **1965,** *87,* 972.

(8) Bartels, M.; Edelüttel-Einhaus, J.; Hoyermann, K. In *Proceedings of the 22nd Symposium (International) on Combustion*; The Combustion Institute: Pittsburgh, 1989; p 1041.

(9) Hippler, H.; Reihs, C.; Troe, J. In *Proceedings of the 23rd Symposium (International) on Combustion*; The Combustion Institute: Pittsburgh, in press.

(10) Emdee, J. L.; Brezinsky, K.; Glassman, I. In *Proceedings of the 23rd Symposium (International) on Combustion*; The Combustion Institute: Pittsburgh, in press.

0022-3654/91/2095-1626$02.50/0

was injected at a high velocity via four quartz capillary tubes and rapidly mixed with the turbulent stream of nitrogen and oxygen. The reacting mixture was convected down a 10-cm-diameter, 100-cm-long quartz tube. To minimize temperature gradients, the tube walls were maintained at the initial reaction temperature by the use of electrical resistance heaters, and the flow rate of the nitrogen carrier gas (and hence the residence time) was adjusted so that the temperature rise due to the conversion of CO to CO_2 did not occur (except for the 1199 K run for *p*-xylene). Because the nitrogen carrier gas made up about 98 mol % of the total flow, any temperature rise due to reactions other than CO conversion to CO_2 was small. The test conditions are shown in Table I.

Temperature measurements were made with a thermocouple, and gas samples were collected with a hot water cooled (≈343 K) stainless steel probe inserted axially into the exit of the reaction tube. Samples were collected at 15 axial positions within the reaction tube. Because a physical sample probe was used, only the detection of stable species was possible. Molecular hydrogen and oxygen were analyzed on-line by using a thermal conductivity detector and a Leeds and Northrup thermomagnetic analyzer, respectively. The samples were also stored in heated (343–373 K) stainless steel loops for analysis afterward using gas chromatography (GC) or gas chromatography/mass spectrometry (GC/MS).

Due to the wide range of molecular weights in the sample gas (C_1's through C_{16}'s), the GC analysis was performed using a unique arrangement involving a Hewlett-Packard 5890A GC fitted with a SGE column switching system. The gas samples were initially injected onto a 30-m J&W Scientific DB-5 capillary column; since the C_1's through C_3's eluted from the column only partially separated, the column flow was diverted from a flame ionization detector (FID) by the column switcher to a second column. The second column was a 10-m Chrompack PoraPLOT Q capillary column fitted with a nickel catalyst methanator (for detector of CO and CO_2) and a second FID. This second column was better suited for separation of small hydrocarbons. Once the C_1–C_3's had entered the second column, the first column flow was transferred back to the first FID. At this point separate carrier gas was flowing through each column, and both detectors were monitored. This arrangement took advantage of the favorable separation characteristics of both columns, shortened analysis time considerably, and prevented the contamination of the PoraPLOT Q and the methanator by heavy hydrocarbons. Peak identification was determined by retention time matching and GC/MS analysis.

Based on calibrations for GC analyzed species, the uncertainty in mole fraction is ±5% for nonaromatic carbon-containing species and ±10% for aromatics, except for the methylbenzyl dimer for which the uncertainty is much higher (maybe ±25%) due to condensation problems with this low vapor pressure species which could not be corrected. The uncertainty in H_2 is ±100 ppm (the resolution of the on-line thermal conductivity analyzer), and ±5% uncertainty is expected for the O_2 measurements. The time from injection of the fuel was calculated by using the probe position and the velocity profile of the flow and is accurate to ±20% based on uncertainties in the carrier gas flow rate and velocity profile. The initial temperature of reaction was determined by using the temperature measured at the point closest to the point of fuel injection. Since the temperature change was small throughout the reaction, little error is expected in assigning this to the initial temperature. The absolute uncertainty in the measured temperature is expected to be ±10 K.

The xylenes and *p*-methylanisole were purchased from Aldrich Chemical Co. with purities greater than 99%. The *p*-tolualdehyde was purchased from Kodak with a purity of greater than 99.5%. The oxygen was from Airco and was over 99.993% pure. The composition of each liquid fuel was confirmed by GC analysis, and each was used without further purification.

Results

The effect of equivalence ratio Φ, as defined in Table I, was studied for *m*- and *p*-xylene by maintaining the initial temperature at about 1155 K and varying Φ from 0.54 to 1.7. The effect of temperature was studied for the para isomer by keeping Φ at about 0.5 and varying the initial temperature from 1093 to 1199 K. In

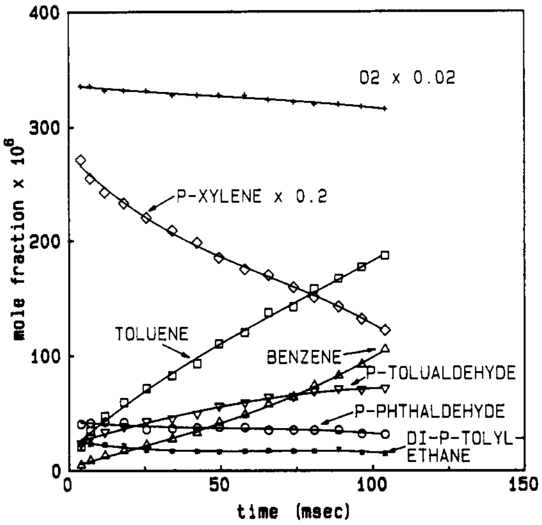

Figure 1. Mole fraction of fuel, oxygen, and intermediates as a function of time for the oxidation of *p*-xylene at an initial temperature of 1155 K, initial fuel mole fraction of 1420 × 10^{-6}, and an equivalence ratio of 0.89.

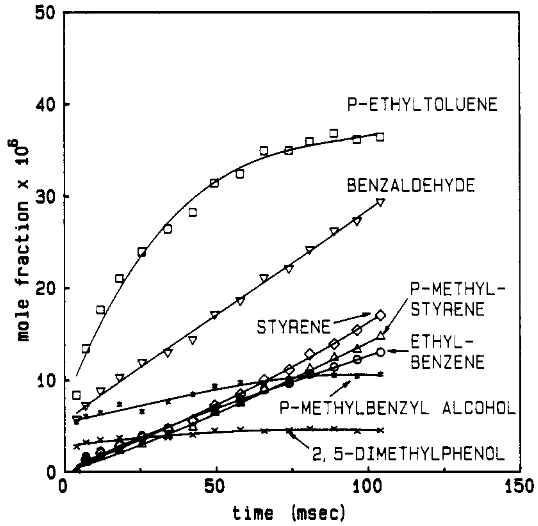

Figure 2. Mole fraction of intermediates as a function of time for the oxidation of *p*-xylene at the conditions of Figure 1.

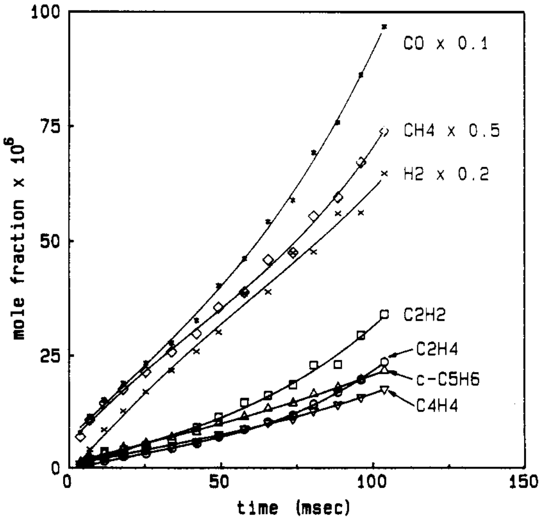

Figure 3. Mole fraction of intermediates as a function of time for the oxidation of *p*-xylene at the conditions of Figure 1.

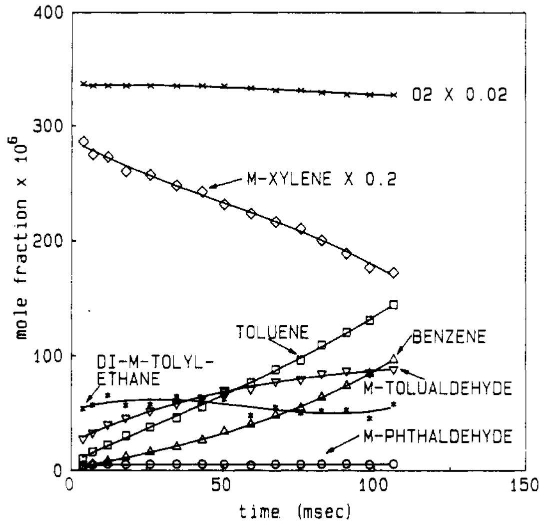

Figure 4. Mole fraction of fuel, oxygen, and intermediates as a function of time for the oxidation of *m*-xylene at an initial temperature of 1155 K, initial fuel mole fraction of 1580×10^{-6}, and an equivalence ratio of 1.0.

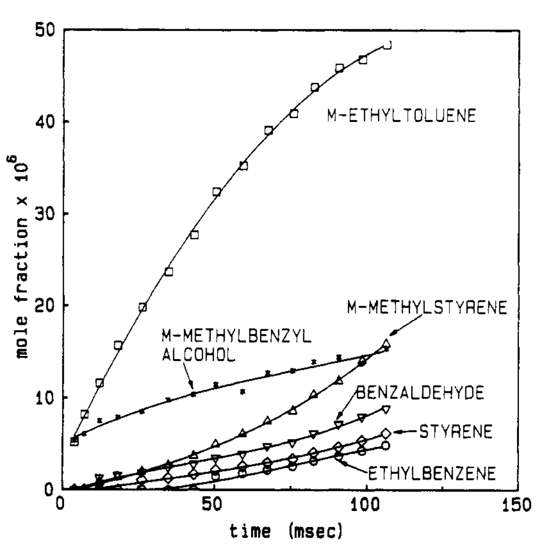

Figure 5. Mole fraction of intermediates as a function of time for the oxidation of *m*-xylene at the conditions of Figure 4.

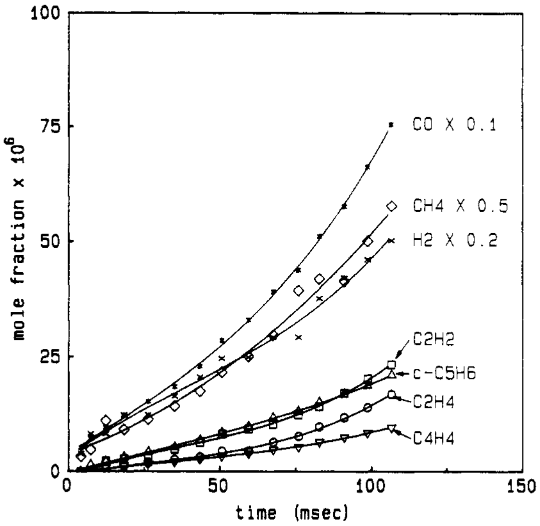

Figure 6. Mole fraction of intermediates as a function of time for the oxidation of *m*-xylene at the conditions of Figure 4.

each case the initial fuel mole fraction was constant at about 1500 ppm, and the oxygen mole fraction was varied to achieve the appropriate stoichiometry. In general, the oxidation mechanisms did not change significantly over the conditions studied so only detailed results for Φ near 1.0 and an initial temperature of 1155 K are presented in Figures 1–6. Where it is useful, selected results from other conditions will be discussed. Further details can be found elsewhere.[11]

As can be seen in Figures 1–6, the major aromatic intermediates (see Figures 7 and 8 for the chemical structures) that were detected for both isomers were benzene, toluene, tolualdehyde ($CH_3C_6H_4CHO$), ethyltoluene ($CH_3C_6H_4C_2H_5$), benzaldehyde (C_6H_5CHO), ethylbenzene ($C_6H_5C_2H_5$), styrene ($C_6H_5C_2H_3$), methylbenzyl alcohol ($CH_3C_6H_4CH_2OH$), methylstyrene ($CH_3C_6H_4C_2H_3$), and the methylbenzyl recombination product, 1,2-ditolylethane ($CH_3C_6H_4CH_2CH_2C_6H_4CH_3$). The major aliphatics detected were methane, acetylene, ethene, cyclopentadiene, and vinylacetylene ($CH_2{=}CH{-}C{\equiv}CH$). CO and H_2 were also major products. Other products not shown included CO_2 (maximum of $\approx$110 ppm), ethane (10 ppm), allene (5 ppm), propyne (10 ppm), butadiene (5 ppm), a linear C_6H_6 believed to be 1,3-hexadien-5-yne (10 ppm), phenol (C_6H_5OH, 10 ppm), cresols ($Ch_3C_6H_4OH$, 10 ppm), and benzyl alcohol ($C_6H_5CH_2OH$, 5 ppm). Only trace amounts, typically less than 5 ppm, of propene, 2-ethynylpropene, methylcyclopentadienes, other xylenes, indene, naphthalene, and phenylacetylene were detected and are also not shown. All of the above species were detected during the oxidation of *m*- and *p*-xylene, and the dialkylated species detected had the same isomeric structure as the parent fuel (i.e., *p*-xylene produced para species and *m*-xylene produced meta species), except for the cresols. GC separation of *m*- and *p*-cresol was poor; however, it was possible to determine that significantly less *o*-cresol than *m*- and *p*-cresol was formed for each fuel. Based on the cresol formation mechanism to be discussed later, the formation of cresol with the isomeric structure of the parent fuel is believed to be favored.

Although all of the above species were detected for each fuel isomer, the formation of phthalaldehyde ($CHOC_6H_4CHO$) was greatly favored for the para isomer when compared to the meta isomer (see Figures 1 and 4). Also, small amounts of dimethylphenol ($(CH_3)_2C_6H_3OH$) (see Figure 2) and ethylbenzaldehyde ($C_2H_5C_6H_4CHO$) (shown later in Figure 12) were detected for the para isomer and not for the meta isomer.

Discussion

Addition reactions involving the aromatic ring were determined to be unimportant compared to reactions involving the side chains based on the following arguments. First of all, hydrogen atom addition to the ring (at a point other than an ipso site) is highly reversible at these temperatures.[12] Furthermore, OH addition is slow compared to side chain hydrogen abstraction.[13] Oxygen atom addition however might be expected to occur and can form either dimethylphenoxy plus H atom or dimethylphenol.[14] Cvetanovic[15] in reviewing lower temperature work favors the former, while work at higher temperatures suggests that the primary addition product of O and an aromatic is a substituted phenol.[16] In either case, since dimethylphenoxy can combine at a fast rate with H atom to form dimethylphenol,[17] one would expect to find dimethylphenols in the oxidation of the xylenes.

For the addition of O atom to *p*-xylene only one dimethylphenol can be formed, namely, 2,5-dimethylphenol, due to the fact that the four available sites on the ring are identical. For the case of *m*-xylene there are three unique sites for the addition of O atom

---

(11) Emdee, J. L. An Experimental and Modeling Study of the High Temperature Oxidation of the Xylenes. Ph.D. Thesis, Mechanical and Aerospace Engineering Department, Princeton University, January 1991.

(12) Nicovich, J. M.; Ravishankara, A. R. *J. Phys. Chem.* **1984**, *88*, 2534.

(13) Madronich, S.; Felder, W. *J. Phys. Chem.* **1985**, *89*, 3556.

(14) Sibener, S. J.; Buss, R. J.; Casavecchia, P.; Hirooka, T.; Lee, Y. T. *J. Chem. Phys.* **1980**, *72*, 4341.

(15) Cvetanovic, R. J. *J. Phys. Chem. Ref. Data* **1987**, *16* (2), 261.

(16) Mulder, P.; Louw, R. *Int. J. Chem. Kinet.* **1988**, *20*, 577.

(17) He, Y. Z.; Mallard, W. G.; Tsang, W. *J. Phys. Chem.* **1988**, *92*, 2196.

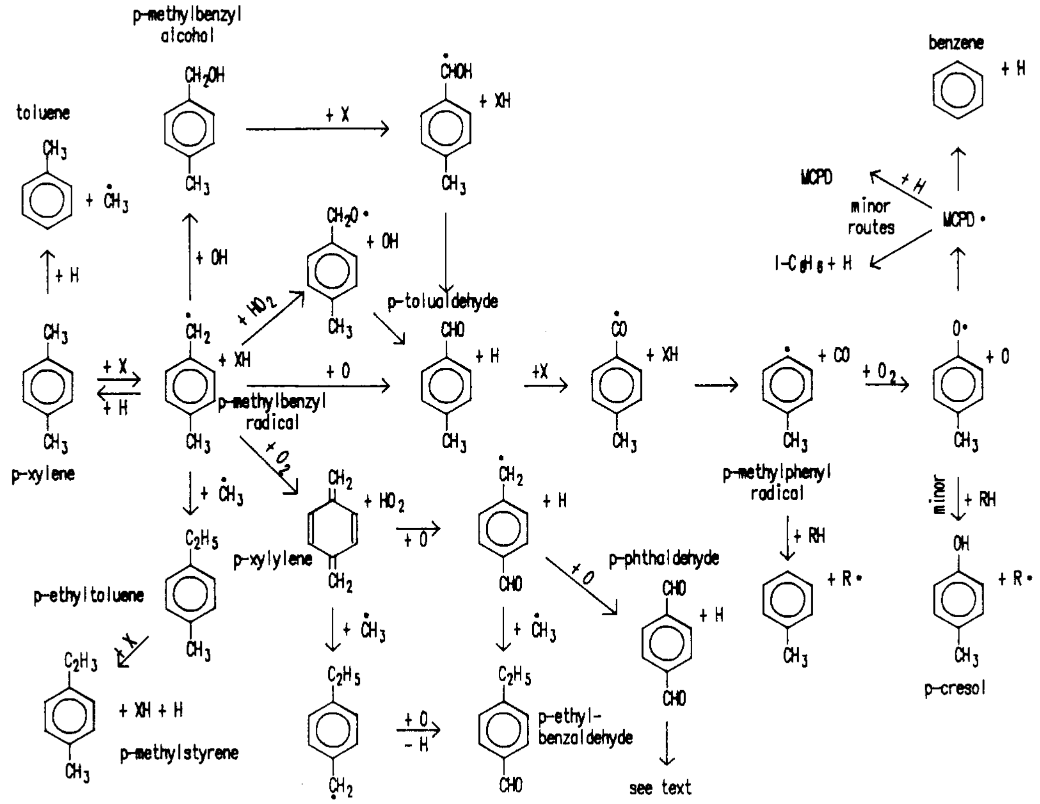

Figure 7. Reaction mechanism for the oxidation of *p*-xylene.

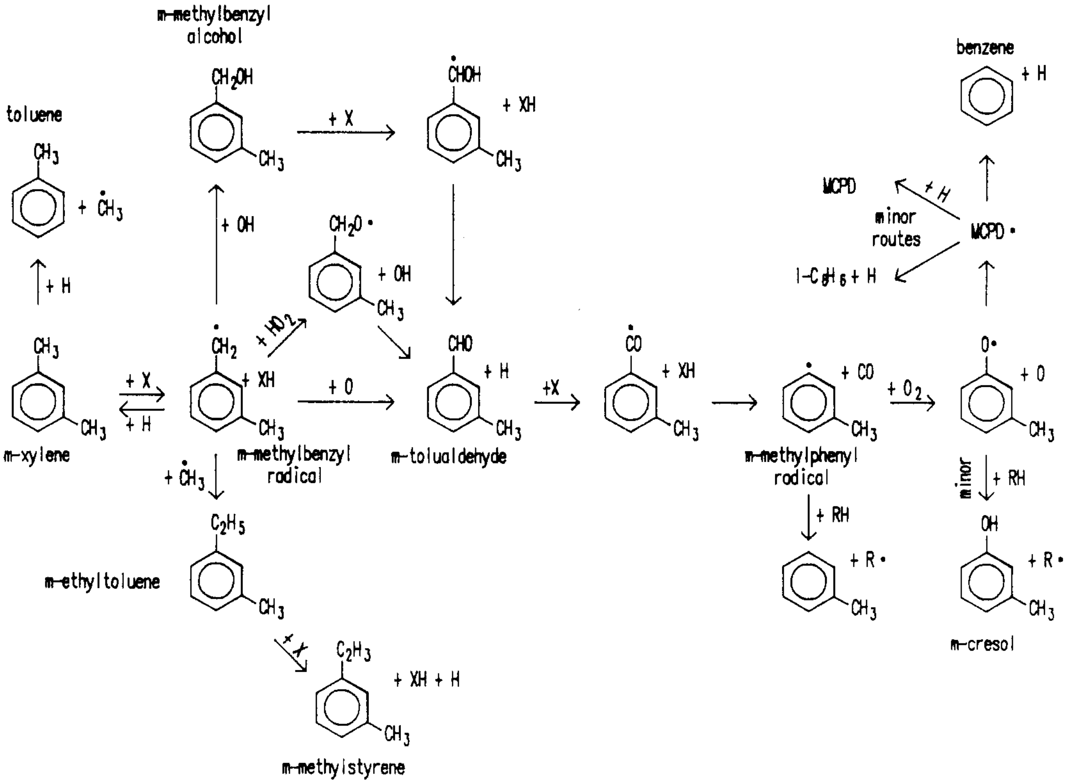

Figure 8. Reaction mechanism for the oxidation of *m*-xylene.

allowing for the production of 2,4-, 2,6-, and 3,5-dimethylphenol with formation of the 2,4-isomer being preferred based on the number of sites and electron density arguments. Only small amounts of 2,5-dimethylphenol were found in the *p*-xylene oxidation (Figure 2), much less than the amount of cresols found during a comparable oxidation of toluene,[3] and unmeasurable amounts of the expected dimethylphenols were found in the *m*-xylene oxidation. These observations can be partially explained by kinetic data[18,19] which suggest that O atom only adds to toluene and benzene but is equally likely to add to the ring or abstract a side chain hydrogen from the xylenes at the temperatures of this study. From the lack of significant amounts of dimethylphenols, it is concluded that addition of O atom is a minor route

---

[18] Nicovich, J. M.; Gump, C. A.; Ravishankara, A. R. *J. Phys. Chem.* **1982**, *86*, 1684.

[19] Nicovich, J. M.; Gump, C. A.; Ravishankara, A. R. *J. Phys. Chem.* **1982**, *86*, 1690.

for the consumption of the fuel.

As previously determined for *p*-xylene,[11,20] the abstraction of a benzylic H forming the methylbenzyl radical, $CH_3C_6H_4CH_2^{\bullet}$ (reaction 1), is expected to be responsible for about 65–75% of the total fuel consumption, and the displacement of a methyl group by H atom producting toluene and methyl (reaction 2) is believed

$$CH_3C_6H_4CH_3 + X \rightarrow CH_3C_6H_4\dot{C}H_2 + XH \qquad (1)$$

$$(X = OH, O, H, O_2, R^{\bullet} \text{ where } R^{\bullet} \text{ is any hydrocarbon radical})$$

$$CH_3C_6H_4CH_3 + H \rightarrow C_6H_5CH_3 + CH_3 \qquad (2)$$

to account for 20–30% of the fuel disappearance. The initial abstraction of a benzylic H is expected to dominate for both isomers because the benzylic C–H bond dissociation energy (BDE) of the meta and para isomers are within 0.2 kcal/mol of each other,[21] and reaction rate data have shown no significant differences due to position of the methyl groups on the ring.[22,23] Reaction 2 is expected to account for the majority of the toluene detected (Figures 1 and 4). The oxidation of toluene has been explored previously,[3] and therefore the fate of the methylbenzyl radical formed in reaction 1 will only be considered in the following discussion.

(*I*) *p-Xylene Mechanism.* The mechanism proposed in Figure 7 suggests that *p*-xylene is consumed by both simultaneous and sequential oxidation of the methyl side chains. The sequential oxidation of the side chains will be considered first.

(*A*) *Sequential Oxidation of Methyl Side Chains.* In this route one side chain is completely oxidized and removed before the other side chain is subject to attack.

(*i*) *p-Tolualdehyde Formation and Consumption.* Once the *p*-methylbenzyl radical is formed from reaction 1, the radical site can be oxidized, analogous to the oxidation of benzyl radical[3,8,9] through reactions 3 and 4 forming *p*-tolualdehyde. Radical–

$$p\text{-}CH_3C_6H_4\dot{C}H_2 + O \rightarrow p\text{-}CH_3C_6H_4CHO + H \qquad (3)$$

$$p\text{-}CH_3C_6H_4CH_2 + HO_2 \rightarrow p\text{-}CH_3C_6H_4CH_2O^{\bullet} + OH \qquad (4)$$

$$p\text{-}CH_3C_6H_4CH_2O^{\bullet} \rightarrow p\text{-}CH_3C_6H_4CHO + H$$

radical reactions are possible since the *p*-methylbenzyl radical is resonantly stabilized and can build up to relatively high concentrations as indicated by the detection of significant amounts of 1,2-di(*p*-tolyl)ethane and *p*-ethyltoluene (Figures 1 and 2). Equilibrium calculations and estimated rate data indicate that 1,2-di(*p*-tolyl)ethane is highly unstable at the temperatures of these studies. Thus, most of that which was detected is thought to have formed in the collection probe by combination of *p*-methylbenzyl radicals which existed in the flow reactor:

$$p\text{-}CH_3C_6H_4\dot{C}H_2 + p\text{-}CH_3C_6H_4\dot{C}H_2 \rightarrow CH_3C_6H_4CH_2CH_2C_6H_4CH_3$$

Furthermore, the only reasonable source of the *p*-ethyltoluene is reaction 5, which again is a radical–radical reaction requiring the

$$p\text{-}CH_3C_6H_4\dot{C}H_2 + CH_3 \rightarrow CH_3C_6H_4C_2H_5 \qquad (5)$$

p-methylbenzyl radical to be present in significant amounts. It is worth noting that radical concentration estimates[11,20] suggest that the methyl radical exists at a level of ≈1 ppm in the flow reactor, making combination reactions in the probe negligible for reaction 5.

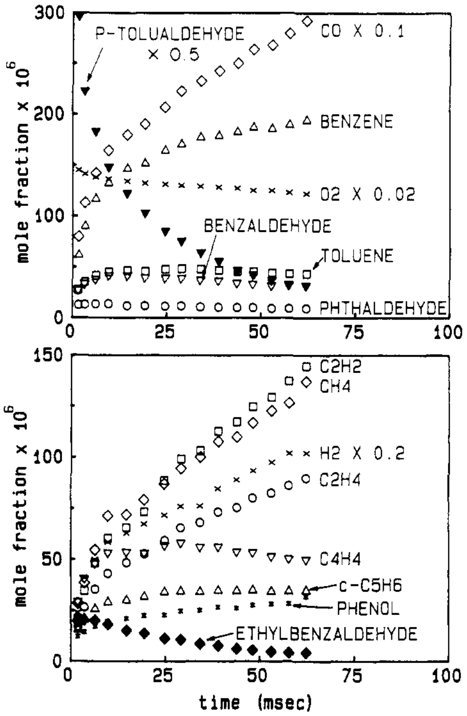

Figure 9. Mole fraction of fuel, oxygen, and intermediates as a function of time for the oxidation of *p*-tolualdehyde at an initial temperature of 1152 K, initial fuel mole fraction of 860 × 10^{-6}, and an equivalence ratio of 1.1.

The *p*-tolualdehyde formed in reactions 3 and 4 can be consumed by abstraction of a hydrogen from the aldehydic side chain forming *p*-methylbenzoyl radical (reaction 6) or from the methyl side chain forming a benzylic radical (reaction 6′). Of course,

$$CH_3C_6H_4CHO + X \rightarrow Ch_3C_6H_4\dot{C}O + XH \qquad (6)$$

$$CH_3C_6H_4CHO + X \rightarrow \dot{C}H_2C_6H_4CHO + XH \qquad (6')$$

displacement of either group by H atom is also possible leading to toluene or benzaldehyde. As will be discussed momentarily, reaction 6 is much faster than reaction 6′. The *p*-methylbenzoyl radical formed in reaction 6 is expected to decompose to CO and *p*-methylphenyl radical[24]

$$p\text{-}CH_3C_6H_4\dot{C}O \rightarrow CO + p\text{-}CH_3C_6H_4^{\bullet} \qquad (7)$$

while the benzylic radical formed in reaction 6′ might further oxidize through reaction 8, analogous to reactions 3 and 4, and

$$p\text{-}\dot{C}H_2C_6H_4CHO + HO_2, O \rightarrow p\text{-}CHOC_6H_4CHO + OH + H, H \qquad (8)$$

form *p*-phthalaldehyde which was detected in the sample gas (Figure 1). Reaction 9 is one possible source of the small amounts of *p*-ethylbenzaldehyde detected.

$$p\text{-}\dot{C}H_2C_6H_4CHO + CH_3 \rightarrow p\text{-}C_2H_5C_6H_4CHO \qquad (9)$$

To determine the relative importance of reactions 6 and 6′, *p*-tolualdehyde was oxidized in the flow reactor at an initial temperature of 1152 K and an equivalence ratio of 1.1. The results are presented in Figure 9 and clearly show that very little *p*-phthalaldehyde and *p*-ethylbenzaldehyde formed. In fact, less *p*-phthalaldehyde was found in the *p*-tolualdehyde oxidation with an initial fuel loading of 860 ppm than was found in the *p*-xylene oxidation where the *p*-tolualdehyde reached only about 75 ppm. Instead, large amounts of CO were formed quickly, suggesting that the aldehydic side chain is much more susceptible to attack than the methyl side chain in agreement with relative rate constants for abstraction of aldehydic and benzylic hydrogens.[22,25] Two immediate conclusions can be drawn from the results of Figure 9. First, if we assume that the distribution of species that make up the radical pool in reactions 6 and 6′ are similar in the

---

(20) Emdee, J. L.; Brezinsky, K.; Glassman, I. Oxidation of *p*-Xylene at 1160–1183 K. Fall Technical Meeting, East. Sect. Combustion Institute, 1988; paper 19.

(21) Hayashibara, K.; Kruppa, G. H.; Beauchamp, J. L. *J. Am. Chem. Soc.* **1986**, *108*, 5441.

(22) Nicovich, J. M.; Thompson, R. L.; Ravishankara, A. R. *J. Phys. Chem.* **1981**, *85*, 2913.

(23) Cui, J. P.; He, Y. Z.; Tsang, W. *J. Phys. Chem.* **1989**, *93*, 724.

(24) Solly, R. K.; Benson, S. W. *J. Am. Chem. Soc.* **1971**, *93*, 1592.

(25) Tsang, W.; Hampson, R. F. *J. Phys. Chem. Ref. Data* **1986**, *15*, 1087.

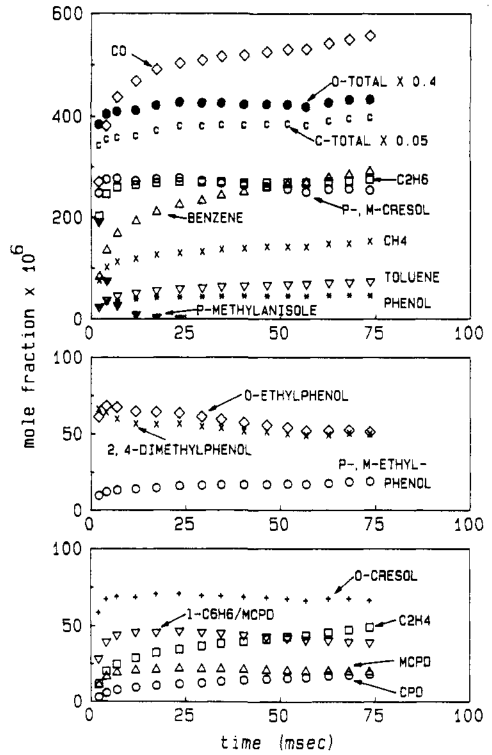

Figure 10. Mole fraction of fuel and intermediates as a function of time for the pyrolysis of *p*-methylanisole at an initial temperature of 1043 K and initial fuel mole fraction of 970 × 10^{-6}.

oxidation of *p*-xylene and *p*-tolualdehyde, then reaction 6 appears to be faster than reaction 6′. Second, the majority of the *p*-phthalaldehyde and *p*-ethylbenzaldehyde formed during the *p*-xylene test must come from a source other than *p*-tolualdehyde. Before discussing the other source, the fate of the *p*-methylphenyl radical from reaction 7 will be considered.

(*ii*) *p-Methylphenyl Radical Reactions.* Similar to the phenyl radical, the *p*-methylphenyl radical can react with molecular oxygen to form *p*-methylphenoxy (reaction 10) or abstract an H from some other hydrocarbon, such as *p*-tolualdehyde or the fuel, to form toluene (reaction 11). Ichimura et al.[26] and Brenner et

$$p\text{-}CH_3C_6H_4^{\bullet} + O_2 \rightarrow p\text{-}CH_3C_6H_4O^{\bullet} + O \qquad (10)$$

$$p\text{-}CH_3C_6H_4^{\bullet} + RH \rightarrow C_6H_5CH_3 + R^{\bullet} \qquad (11)$$

al.[27] have found evidence that the ortho isomer of the methylphenyl radical rearranges to benzyl radical via a 1,3-hydrogen shift, but they found no indication that the meta and para isomers formed benzyl. Estimating the rates of reactions 10 and 11 using values for similar reactions involving phenyl radical[28,29] and using the concentration of O_2 and *p*-xylene (RH) for the test conditions of T_0 = 1155 K and Φ = 0.89 reveals that reactions 10 and 11 are equally likely to occur.

(*iii*) *p-Methylphenoxy Radical Reactions.* To reveal the fate of the *p*-methylphenoxy radical of reaction 10, *p*-methylanisole (p-$CH_3C_6H_4OCH_3$) was pyrolyzed in the flow reactor at 1043 K with an initial fuel loading of 970 ppm. *p*-Methylanisole is known to decompose almost exclusively at this temperature by homolysis of the O–CH_3 bond to produce methyl radical and *p*-methylphenoxy radical:[30]

$$p\text{-}Ch_3C_6H_4OCH_3 \rightarrow p\text{-}CH_3C_6H_4O^{\bullet} + CH_3$$

The pyrolysis results are shown in Figure 10 and reveal that the main products of decompositions were CO, benzene, *p*-cresol, methane, and ethane. Minor products included ethylphenols, 2,4-dimethylphenol, toluene, phenol, *o*-cresol, methylcyclopentadienes (MCPD's), a linear C_6H_6 (the same species that was found during the xylene tests), ethene, and cyclopentadiene (CPD). Except for a gradual increase in benzene and CO levels, the composition of the product gases changed very little after the fuel was consumed. A reaction mechanism is postulated in Appendix A. Although admittedly speculative, this mechanism is consistent with the present experimental data and available literature data.

The formation of methylcyclopentadienyl (MCPD•)

$$p\text{-}CH_3C_6H_4O^{\bullet} \rightarrow CO + MCPD^{\bullet} \qquad (12)$$

is believed to occur by analogy with the decomposition of phenoxy, $C_6H_5O^{\bullet}$, to CO and cyclopentadienyl, CPD•.[31,32] Considering the mole fraction of CO at the point of fuel disappearance, it appears that reaction 12 accounts for approximately 50% of the *p*-methylphenoxy decomposition, while the phenols formed account for the remaining *p*-methylphenoxy units. The primary phenol, *p*-cresol (p-$CH_3C_6H_4OH$), is most likely formed by

$$p\text{-}CH_3C_6H_4O^{\bullet} + RH \rightarrow p\text{-}CH_3C_6H_4OH + R^{\bullet} \qquad (13)$$

Reaction 13 accounts for 30% of the *p*-methylphenoxy disappearance based on the amount of *p*-cresol and its decomposition products, phenol and *p*-ethylphenol; see reactions A8–A10 in Appendix A. Due to the lack of separation of the *m*- and *p*-cresol and the *m*- and *p*-ethylphenol during the GC analysis, it was assumed that the each peak was due to the para species since the formation of the meta species was unlikely. See Appendix A for further discussion of the various phenols formed.

3-Methyl-2,4-cyclopentadien-1-yl is the most likely MCPD• isomer to form in reaction 12 based on the phenoxy decomposition mechanism proposed in refs 31 and 32; however, the stable MCPD's are known to isomerize to both 1-methyl-1,3-cyclopentadiene and 2-methyl-1,3-cyclopentadiene.[33] Indeed two MCPD GC peaks were identified; unfortunately, poor separation of one of the MCPD's from the 1-C_6H_6 prevented quantitative integration of these peaks. Qualitatively, the two MCPD peaks were approximately equal in size. In any event the total yield of the MCPD's (formed by reaction A6) and their reaction products (CPD and 1-C_6H_6 through reactions A5 and A7) accounts for only about 15% of the MCPD• generated by reaction 12 as indicated by the CO mole fraction; most of the MCPD• rearranges to benzene:

$$MCPD^{\bullet} \rightarrow c\text{-}C_6H_7^{\bullet} \rightarrow C_6H_6 + H \qquad (14)$$

This reaction explains the large amount of benzene in Figure 10 and has been suggested previously.[34-36] See Appendix A for more discussion of the mechanism for this reaction. Reaction 14 appears to be the major reaction path of the MCPD• since the total mole fractions of benzene and toluene (via reaction A11) account for over 60% of the MCPD• formed. Because benzene and CO were major intermediates during the *p*-tolualdehyde oxidation (Figure 9), the *p*-tolualdehyde results support the formation of benzene from MCPD•. Further oxidation of the benzene was possible in those test due to the presence of oxygen as evidenced by the formation of ring destruction products (e.g., C_2H_2 and C_4H_4).

Thus, 75% of the MCPD• can be accounted for by the above paths at the point of fuel disappearance. The remaining 25% could not be reconciled; in fact, a comparison of the carbon total and the oxygen total in Figure 10 shows that the carbon balance is

---

(26) Ichimura, T.; Mori, Y.; Sumitani, M.; Yoshihara, K. *J. Chem. Phys.* **1986**, *84*, 1943.

(27) Brenner, D. M.; Smith, G. P.; Zare, R. N. *J. Am. Chem. Soc.* **1976**, *98*, 6707.

(28) Lin, C.-Y.; Lin, M. C. Kinetics of the C_6H_5 + O_2 Reaction. Fall Technical Meeting, East. Sect. Combustion Institute, 1987; paper 7.

(29) Fahr, A.; Stein, S. E. *J. Phys. Chem.* **1988**, *92*, 4951.

(30) Suryan, M. M.; Kafafi, S. A.; Stein, S. E. *J. Am. Chem. Soc.* **1989**, *111*, 4594.

(31) Lin, C.-Y.; Lin, M. C. *J. Phys. Chem.* **1986**, *90*, 425.

(32) Colussi, A. J.; Zabel, F.; Benson, S. W. *Int. J. Chem. Kinet.* **1977**, *9*, 161.

(33) McLean, S.; Haynes, P. *Tetrahedron* **1965**, *21*, 2329.

(34) Spielmann, R.; Cramers, C. A. *Chromatographia* **1972**, *5*, 295.

(35) Mackie, J. C.; Doolan, K. R.; Nelson, P. F. *J. Phys. Chem.* **1989**, *93*, 664.

(36) Ritter, E. R.; Bozzelli, J. W.; Dean, A. M. *J. Phys. Chem.* **1990**, *94*, 2493.

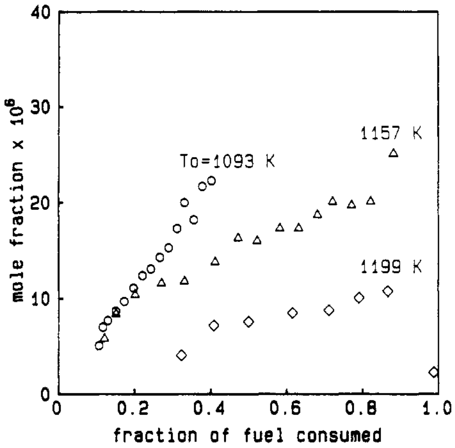

Figure 11. Mole fraction of *p*- and *m*-cresols formed during the oxidation of *p*-xylene as a function of extent of reaction for different temperatures and an equivalence ratio near 0.5.

lower by about 10%. Furthermore, both show that near the beginning of the reaction a deficit in carbon and oxygen exist. These discrepancies could be due to uncertainties in the calibration of the GC, but the following discussion should be considered. This behavior is similar to that found during the pyrolysis of phenol where the major products were observed to be CO and CPD.[37] The amount of CPD detected was less than that predicted by the CO levels leading to the conclusion that the CPD• radical was combining with phenoxy to form low vapor pressure products that were unable to be sampled by the water-cooled collection probe. A similar situation might be occurring to some extent for the *p*-methylanisole pyrolysis in which abundant amounts of *p*-methylphenoxy and MCPD• are present. This would explain (1) the lack of agreement between the carbon and oxygen balances, (2) the deficit in both carbon and oxygen early in the reaction period when the *p*-methylphenoxy is most abundant, and (3) the unaccounted for MCPD•.

From the *p*-methylanisole results it is concluded that the two major consumption routes for the *p*-methylphenoxy radical formed during the *p*-xylene oxidation (reaction 10) are decomposition to MCPD• (reaction 12), which forms primarily benzene (reaction 14), and the formation of *p*-cresol (reaction 13). As discussed earlier, the formation of MCPD• was favored during the *p*-methylanisole pyrolysis. Because reaction 12 is expected to be a high activation energy process[31] compared to reaction 13, the formation of MCPD• is expected to dominate even further as the temperature increases from the test conditions of the *p*-methylanisole pyrolysis (1043 K) to the conditions of the *p*-xylene test (1100–1200 K). Indeed, a comparison of the *p*-cresol (and *m*-cresol) profiles for three *p*-xylene oxidations at similar equivalence ratios (see Figure 11) indicates that the formation rate of *p*-cresol is decreased as the temperature is increased. The cresol profiles are presented as a function of extent of reaction so that a change in mole fraction due simply to an accelerated rate of fuel consumption will not be a factor. It should be noted that the formation of *p*-cresol was greatly favored over *o*-cresol, further suggesting that the major source of the cresol was reaction 13 and not O atom addition to toluene[3] which would have resulted in a more even distribution of the cresol isomers. When the benzene mole fractions were compared for different temperatures, no dependence on temperature was found. Based on the much larger mole fraction of benzene compared to that of cresol, it is possible that the benzene formation route accounted for such a large majority of the *p*-methylphenoxy decomposition that any temperature effect was only visible in the *p*-cresol profile.

The oxidation reactions of benzene[1,2] account for the rapid formation of the cyclopentadiene, the C_4's, and the C_2's as the xylene is consumed. Thus, the mechanism describing the sequential oxidation of the methyl side chains is complete and the simultaneous oxidation mechanism, in which both side chains are attacked before the removal of the first chain, must now be considered.

(*B*) *Simultaneous Oxidation of the Methyl Side Chains.* As stated earlier, the *p*-tolualdehyde oxidation experiments showed that *p*-tolualdehyde was not the major source of the *p*-phthalaldehyde detected during the *p*-xylene oxidation tests. Evidence will be presented here that suggests that the *p*-phthalaldehyde is formed from the intermediate species *p*-xylylene (3,6-bis(methylene)-1,4-cyclohexadiene or *p*-$H_2C{=}C_6H_4{=}CH_2$; see Figure 7 for the chemical structure).

(*i*) *p-Xylylene Formation.* *p*-Xylylene can be formed by the abstraction of an H from the second methyl side chain of *p*-methylbenzyl radical:

$$CH_3C_6H_4\dot{C}H_2 + O_2 \rightarrow p\text{-}H_2C{=}C_6H_4{=}CH_2 + HO_2 \qquad (15)$$

Based on the following bond strength arguments, an oxygen molecule is expected to be the sole abstraction agent in reaction 15 while radicals are expected to play the major role for abstraction of the first H (reaction 1). Once the first benzylic H is abstracted (C–H BDE = 87.6 kcal/mol[21]), the C–H BDE of the second methyl group drops dramatically to about 62 kcal/mol, using the following heats of formation at 298 K: ΔH_f(*p*-xylene) = 4.3 kcal/mol,[38] $\Delta H_f(p\text{-}CH_3C_6H_4CH_2^\bullet)$ = 39.8 kcal/mol,[21] and ΔH_f(*p*-xylylene) = 50 kcal/mol.[39] The assumption was made that the structure for *p*-xylylene shown in Figure 7 will be formed when the second H is removed and not a biradical.[39] Considering that reaction 1 involving O_2 is endothermic by 38 kcal/mol, a lowering of the C–H bond energy in the second methyl group can lower the activation energy for the rate of abstraction by O_2 and cause the reaction rate to be faster (see Appendix B for further discussion). Due to the exothermicity of abstraction by radicals though, any lowering of the C–H BDE will have only a small effect on the rate of abstraction of the second H by a radical when compared to the first H. Instead of abstracting the second H, radicals are more likely to react with the radical site on *p*-methylbenzyl such as in reactions 3, 4, 5, and 16. Reaction 16 is suggested by analogy with the reaction of OH and benzyl radical.[3,9]

$$p\text{-}CH_3C_6H_4\dot{C}H_2 + OH + M \rightarrow p\text{-}CH_3C_6H_4CH_2OH + M \qquad (16)$$

Polymerization of *p*-xylylene could also occur,[40] although concentration considerations probably preclude any significant extent of polymerization. High boiling point polymers beyond the dimer, if formed, would be expected to condense onto the cool walls of the sample probe and be undetected. Although the carbon balance from the GC agreed with the fuel flow rate within experimental uncertainty (indicating no significant loss of intermediates), the probe was lightly coated with a glossy substance which could not be identified.

(*ii*) *p-Phthalaldehyde Formation.* Since *p*-tolualdehyde was not the source of the *p*-phthalaldehyde as indicated earlier, most of the *p*-phthalaldehyde detected during the *p*-xylene oxidation is thought to result from oxidation of the methylene groups of *p*-xylylene:

$$p\text{-}H_2C{=}C_6H_4{=}CH_2 + O \rightarrow p\text{-}\dot{C}H_2C_6H_4CHO + H \qquad (17)$$

$$p\text{-}\dot{C}H_2C_6H_4CHO + HO_2, O \rightarrow p\text{-}CHOC_6H_4CHO + OH + H, H \qquad (8)$$

Because the side chains of *p*-xylylene are double bonded to the ring, reaction 17 is expected to involve O atom, and not HO_2, as determined by the rates of the analogous reactions of O and HO_2 with the double bond of ethene.[25]

Evidence that *p*-xylylene was the precursor to the formation of the *p*-phthalaldehyde can be found by considering the distinctly

---

[37] Lovell, A. B.; Brezinsky, K.; Glassman, I. *Int. J. Chem. Kinet.* **1989**, *21*, 547.

[38] Burcat, A. In *Combustion Chemistry*; Gardiner Jr., W. C., Ed.; Springer-Verlag: New York, 1984; Appendix C.

[39] Pollack, S. K.; Raine, B. C.; Hehre, W. J. *J. Am. Chem. Soc.* **1981**, *103*, 6308.

[40] Errede, L. A.; Cassidy, J. P. *J. Phys. Chem.* **1963**, *67*, 73.

lower concentration of *m*-phthalaldehyde detected during the *m*-xylene oxidation test (see Figures 1 and 4). Pollack et al.[39] showed that the C–H bonds on the second methyl group of *m*-methylbenzyl radical were not measurably weaker than the parent *m*-xylene C–H bonds, a result that is consistent with the formation of a biradical[41] and not a methylenic structure as suggested for *p*-xylylene. Thus, for the meta isomer, reactions such as reaction 3 and 4 would be faster than reaction 15 and the small amount of *m*-phthalaldehyde detected is probably formed by reactions 6′ and 8.

For the pyrolysis of *p*-xylene, Errede and Cassidy[40] reported that the formation of *p*-xylylene from *p*-methylbenzyl radical was a heterogeneous reaction catalyzed by carbonaceous material on the postpyrolysis zone walls at temperatures as low as 573 K. Because the *p*-xylene experiments presented here were performed under very dilute conditions (see Table I) and in the presence of oxygen, the hot quartz reaction tube was never coated with carbonaceous material. The cooled collection probe however was coated after each test, but any *p*-xylylene that may have formed by probe wall reactions could have led to only a fraction of the detected *p*-phthalaldehyde (via reactions 17 and 8) since the mole fractions of the O atom and HO_2 were previously estimated to be much less than 1 ppm.[11,20] It is expected that, rather than forming *p*-xylylene, most of the *p*-methylbenzyl radical that enters the probe combines to form 1,2-di(*p*-tolyl)ethane as mentioned earlier.

(*iii*) *p-Ethylbenzaldehyde Formation.* As will be argued shortly, the detection of *p*-ethylbenzaldehyde (p-$C_2H_5C_6H_4CHO$) also supports the presence of *p*-xylylene.

The results of the *p*-tolualdehyde oxidation study showed that *p*-ethylbenzaldehyde was an intermediate (Figure 9), but not in nearly high enough concentrations to indicate that it was a primary product of the *p*-tolualdehyde. It might be conceivable that the *p*-ethylbenzaldehyde could have formed from oxidation of the methyl group of *p*-ethyltoluene (p-$CH_3C_6H_4C_2H_5$) which was formed by reaction 5. However, the most probable reaction of the *p*-ethyltoluene is abstraction of an H from the ethyl group to eventually form *p*-methylstyrene (reaction 18), which was indeed

$$p\text{-}CH_3C_6H_4C_2H_5 + X \rightarrow p\text{-}CH_3C_6H_4C_2H_3 + XH + H \qquad (18)$$

detected in the sample gas. This is similar to the formation of styrene from ethylbenzene.[4] Futhermore, since an equivalent amount of the appropriate ethyltoluene isomer was found in each xylene experiment, the lack of detection of *m*-ethylbenzaldehyde during the *m*-xylene oxidation tests rules out oxidation of the methyl group of ethyltoluene. Thus, it is concluded that the major path for formation of *p*-ethylbenzaldehyde is methyl addition to the p-$\dot{C}H_2C_6H_4CHO$ radical, formed in reaction 17 (not reaction 6′), before further oxidation by reaction 8 can occur:

$$p\text{-}\dot{C}H_2C_6H_4CHO + CH_3 \rightarrow p\text{-}C_2H_5C_6H_4CHO \qquad (9)$$

Another possible route is through methyl addition to *p*-xylylene followed by oxidation of the remaining radical site:

$$p\text{-}H_2C{=}C_6H_4{=}CH_2 + CH_3 \rightarrow p\text{-}C_2H_5C_6H_4\dot{C}H_2 \qquad (19)$$

$$p\text{-}C_2H_5C_6H_4\dot{C}H_2 + HO_2,\ O \rightarrow p\text{-}C_2H_5C_6H_4CHO + OH + H,\ H \qquad (20)$$

(*iv*) *p-Phthalaldehyde Reactions.* The only remaining steps to consider are the consumption of the *p*-phthalaldehyde. These should be similar to the consumption of the *p*-tolualdehyde in that reactions 21–24 are proposed:

$$p\text{-}CHOC_6H_4CHO + X \rightarrow p\text{-}CHOC_6H_4\dot{C}O + XH \qquad (21)$$

$$p\text{-}CHOC_6H_4\dot{C}O \rightarrow p\text{-}CHOC_6H_4{}^{\bullet} + CO \qquad (22)$$

$$p\text{-}CHOC_6H_4{}^{\bullet} + RH \rightarrow C_6H_5CHO + R^{\bullet} \qquad (23)$$

$$p\text{-}CHOC_6H_4{}^{\bullet} + O_2 \rightarrow p\text{-}CHOC_6H_4O^{\bullet} + O \qquad (24)$$

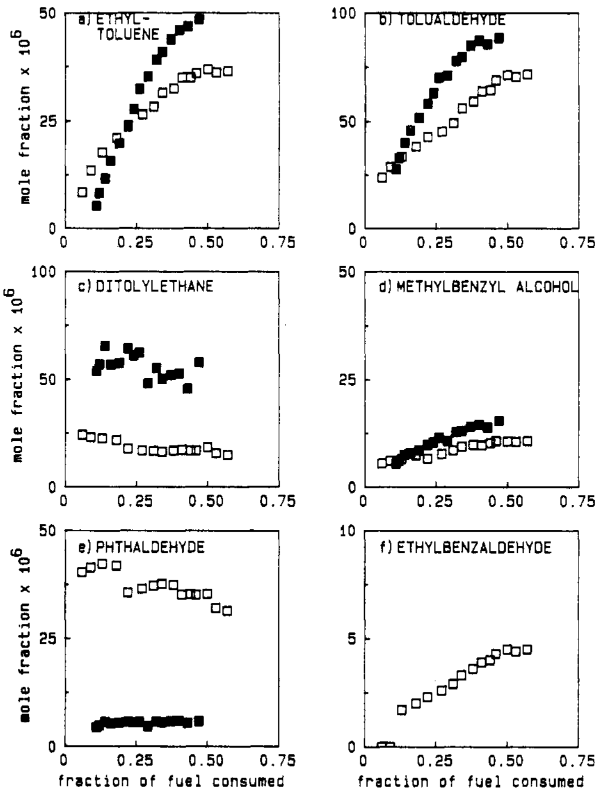

Figure 12. Mole fraction of intermediates formed by reactions involving (a–d) methylbenzyl radical and (e–f) xylylene as a function of extent of reaction. ■ = *m*-xylene oxidation at T_0 = 1155 K, Φ = 1.0, and initial fuel mole fraction of 1580 × 10^{-6}. □ = *p*-xylene oxidation at T_0 = 1155 K, Φ = 0.89, and initial fuel mole fraction of 1420 × 10^{-6}.

Indeed, benzaldehyde (reaction 23) was found in the sample gas (Figure 2) in higher concentrations than found for the *m*-xylene oxidation (Figure 5) in which less phthalaldehyde was present. However, because benzaldehyde can be formed from toluene oxidation, this result may not be significant. Lastly, the fate of the p-$CHOC_6H_4O^{\bullet}$ radical is unclear, but by analogy with reaction 12 one might expect

$$p\text{-}CHOC_6H_4O^{\bullet} \rightarrow c\text{-}\dot{C}_5H_4CHO + CO \qquad (25)$$

$$c\text{-}\dot{C}_5H_4CHO \rightarrow c\text{-}C_5H_5\dot{C}O \rightarrow CPD^{\bullet} + CO \qquad (26)$$

where reaction 26 would involve a hydrogen shift from the aldehyde to the C_5 ring.

(*II*) *m-Xylene Mechanism.* Due to the lack of a simultaneous oxidation route involving *m*-xylylene, the proposed oxidation mechanism of *m*-xylene shown in Figure 8 is less complex than the mechanism for *p*-xylene. As was discussed, less *m*-phthalaldehyde was detected compared to the amount of *p*-phthalaldehyde found during the *p*-xylene tests and no *m*-ethylbenzaldehyde was detected (Figure 12e–f). Both of these intermediates were argued to be indications that xylylene was being formed during the *p*-xylene oxidation and not during the *m*-xylene oxidation. Also, heat of formation measurements[39] indicated that there was no weakening of the C–H bonds in *m*-methylbenzyl radical due to the structural constraints that required *m*-xylylene to exist as a biradical.[41]

Considering Figures 1–6 it is apparent that, with the few exceptions previously noted, the reaction products of *m*-xylene are very similar to the products of *p*-xylene. All of the reactions previously described for the sequential oxidation mechanism of the para isomer can equally apply to the meta isomer. Therefore, a description of the *m*-xylene mechanism would be redundant and the mechanism shown in Figure 8 will be considered to be self-explanatory.

(*III*) *Comparison of Methylbenzyl Radical Concentrations.* Since the absence of reaction 15 constitutes one fewer sink for the *m*-methylbenzyl radical, one might expect that the methyl-

---

[41] Lejeune, V.; Despres, A.; Migirdicyan, E.; Baudet, J.; Bethier, G. *J. Am. Chem. Soc.* **1986**, *108*, 1853.

benzyl radical concentration would be higher during a *m*-xylene oxidation than for an equivalent *p*-xylene oxidation. Due to the nature of the sampling system, it was not possible to measure the radical mole fractions, but it was possible to measure the intermediates that were direct products of methylbenzyl reactions such as

$$CH_3C_6H_4\dot{C}H_2 + O \rightarrow CH_3C_6H_4CHO + H \qquad (3)$$

$$CH_3C_6H_4\dot{C}H_2 + HO_2 \rightarrow CH_3C_6H_4CH_2O^{\bullet} + OH \qquad (4)$$

$$CH_3C_6H_4CH_2O^{\bullet} \rightarrow CH_3C_6H_4CHO + H$$

$$CH_3C_6H_4\dot{C}H_2 + CH_3C_6H_4\dot{C}H_2 \rightarrow CH_3C_6H_4CH_2CH_2C_6H_4CH_3$$

$$CH_3C_6H_4\dot{C}H_2 + CH_3 \rightarrow CH_3C_6H_4C_2H_5 \qquad (5)$$

$$CH_3C_6H_4\dot{C}H_2 + OH + M \rightarrow CH_3C_6H_4CH_2OH + M \qquad (16)$$

Note that the *p*-prefix has been removed since these reactions are expected to occur for both isomers. Figure 12a–d shows a comparison of the mole fraction of the products of the above reactions as a function of extent of fuel consumption. For the same extent of reaction, the rate of production of these products was greatest during the oxidation of *m*-xylene. If it is reasonably assumed that the reaction rates are negligibly affected by the position of the alkyl groups on the ring, as argued earlier, then the increases in production rate shown in Figure 12 are primarily due to a greater concentration of methylbenzyl radical during the *m*-xylene oxidation. Furthermore, this trend is believed to be a direct result of the greater stability of *m*-methylbenzyl radical to consumption by reaction 15.

Conclusion

The reaction mechanisms of *m*- and *p*-xylene are very similar except for the formation and consumption reactions of *p*-xylylene in the oxidation of *p*-xylene. The role of *p*-xylylene was not included in previous low-temperature mechanisms and is probably not important at low temperatures due to the expected high activation energy of the endothermic formation reaction (reaction 15). In fact, the *p*-xylene tests revealed larger concentrations of 1,2-di(*p*-tolyl)ethane and greater rates of formation of *p*-ethyltoluene, *p*-methylbenzyl alcohol, and *p*-tolualdehyde at the lower temperatures (1093 K) than at the higher temperatures (1199 K) for similar extents of fuel consumption (just as Figure 12 showed for the meta isomer as compared to the para isomer for the same temperature). The most likely explanation is that, because reaction 15 is relatively slower at the low temperatures compared to the competing radical recombination reactions, the *p*-methylbenzyl radical reaches a higher concentration.

It is interesting to note that, when the oxidations of benzene and toluene were studied, it was found that in order to achieve the same extent of reaction the initial temperature of toluene had to be 100 K higher than that for benzene[42] in spite of the fact that the benzylic C–H bonds of toluene are about 13 kcal/mol weaker than the C–H bonds of benzene.[43] The difference in reactivity was suggested to be a result of the resonant stability, and hence unreactivity, of the benzyl radical which bottlenecked the toluene oxidation reaction. When the rates of fuel consumption for the *m*- and *p*-xylene are compared, as in Figure 13, it is seen that *p*-xylene reacts faster than *m*-xylene for the leaner condition when more oxygen is present. It is apparent that by having available an additional channel for the decomposition of the *p*-methylbenzyl radical, reaction 15, the reaction sequence is not bottlenecked as much at the methylbenzyl stage.

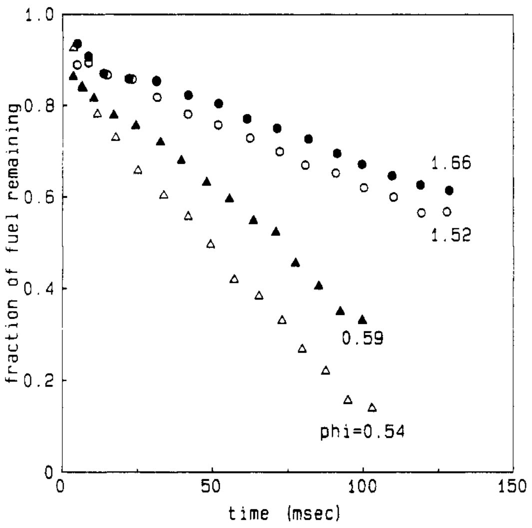

Figure 13. Fraction of fuel remaining for the oxidation of *m*-xylene (filled symbols) and *p*-xylene (open symbols) as a function of time for an initial temperature of about 1155 K. The faster rate of reaction of *p*-xylene is apparent.

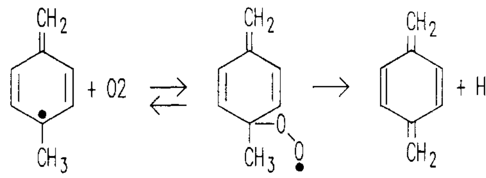

Figure 14. Alternate reaction scheme for $O_2 + CH_3C_6H_4CH_2^{\bullet} \rightarrow$ xylylene + HO_2.

Acknowledgment. The technical support of J. Sivo and P. Michniewicz is gratefully acknowledged as well as insightful discussions with M. B. Colket III. Research was sponsored by the Air Force Office of Scientific Research, Air Force Systems Command, USAF, under Grant AFOSR-890034. Additional research support was provided by the Fundamental Interactions Branch of the Division of Chemical Services, Office of Basic Energy Sciences of the Department of Energy, through Grant DE-FG02-86ER13554.

Appendix A

The following simplified mechanism is proposed to explain the *p*-methylanisole pyrolysis results shown in Figure 10:

$$p\text{-}CH_3C_6H_4OCH_3 \rightarrow p\text{-}CH_3C_6H_4O^{\bullet} + CH_3 \qquad (A1)$$

$$p\text{-}CH_3C_6H_4O^{\bullet} \rightarrow CO + MCPD^{\bullet} \qquad (12)$$

$$p\text{-}CH_3C_6H_4O^{\bullet} + RH \rightarrow p\text{-}CH_3C_6H_4OH + R^{\bullet} \qquad (13)$$

$$p\text{-}CH_3C_6H_4O^{\bullet} + CH_3 \rightarrow \text{2,4-dimethylphenol} \qquad (A2)$$

$$CH_3 + CH_3 + M \rightarrow C_2H_6 + M \qquad (A3)$$

$$CH_3 + RH \rightarrow CH_4 + R^{\bullet} \qquad (A4)$$

$$MCPD^{\bullet} \rightarrow c\text{-}C_6H_7^{\bullet} \rightarrow C_6H_6 + H \qquad (14)$$

$$MCPD^{\bullet} \rightarrow c\text{-}C_6H_7^{\bullet} \rightarrow 1\text{-}C_6H_6 + H \qquad (A5)$$

$$MCPD^{\bullet} + H \rightarrow MCPD \qquad (A6)$$

$$MCPD + H \rightarrow CPD + CH_3 \qquad (A7)$$

$$p\text{-}CH_3C_6H_4OH + H \rightarrow C_6H_5OH + CH_3 \qquad (A8)$$

$$p\text{-}CH_3C_6H_4OH + X \rightarrow p\text{-}\dot{C}H_2C_6H_4OH + XH \qquad (A9)$$

$$p\text{-}\dot{C}H_2C_6H_4OH + CH_3 \rightarrow p\text{-}C_2H_5C_6H_4OH \qquad (A10)$$

$$C_6H_6 + CH_3 \rightarrow C_6H_5CH_3 + H \qquad (A11)$$

---

[42] Brezinsky, K.; Lovell, A. B.; Glassman, I. *Combust. Sci. Technol.* **1990**, *70* (1–3), 33.

[43] McMillen, D. F.; Golden, D. M. *Annu. Rev. Phys. Chem.* **1982**, *33*, 493.

$$C_2H_6 + X \rightarrow C_2H_5 + XH \qquad (A12)$$

$$C_2H_5 + M \rightarrow C_2H_4 + H + M \qquad (A13)$$

Reaction A2 actually takes place through a dimethylcyclohexadienone intermediate[44] and is responsible for the dimethylphenol detected. The mechanism does not explain the formation of the *o*-ethylphenol and *o*-cresol which might be formed by scrambling of the position of the alkyl groups on the ring or possibly by ethyl/methyl addition to phenol at the ortho site.

Methyl addition to benzene (reaction A11) is expected to be the major source of toluene rather than

$$p\text{-}CH_3C_6H_4OH + H \rightarrow C_6H_5CH_3 + OH$$

because H atoms are more likely to displace the methyl of cresol by reaction A8.[17] The abundance of methyl radicals in this system causes methyl addition reactions such as reaction A11 to be favorable compared to the reverse reactions.

Reactions 14 and A5 may actually include formation of cyclopentadienylmethyl radical (c-$C_5H_4CH_2^\bullet$) and a bicyclo intermediate (bicyclo[3.1.0]hex-2-en-4-yl) before formation of cyclohexadienyl (c-$C_6H_7^\bullet$).[36] Using QRRK calculations to study reactions of chlorobenzene in hydrogen at 1050–1275 K and 1-atm pressure, Ritter et al.[3]16 found that MCPD$^\bullet$ rapidly equilibrates with benzene and H atom and that equilibrium strongly favors benzene formation. Furthermore, their calculations indicated very little formation of the linear C_6 species. Both conclusions are supported experimentally by the *p*-methylanisole results shown in Figure 10.

Appendix B

The extent to which the activation energy for the reaction

$$p\text{-}CH_3C_6H_4\dot{C}H_2 + O_2 \rightarrow p\text{-}H_2C{=}C_6H_4{=}CH_2 + HO_2 \quad (\Delta H = +12.7\ \text{kcal/mol}) \quad (15)$$

is lowered, relative to the activation energy for reaction 1 involving O_2

$$p\text{-}CH_3C_6H_4CH_3 + O_2 \rightarrow p\text{-}CH_3C_6H_4\dot{C}H_2 + HO_2 \quad (\Delta H = +38.0\ \text{kcal/mol}) \quad (1_{O2})$$

depends on the structure of the transition state. If it is assumed for these endothermic reactions that the activation energy for abstraction is lowered by the full drop in the BDE, about 25 kcal/mol, then an estimate for the rate of reaction 15 could be made from the rate constant for reaction 1_{O2}. Unfortunately, this latter rate constant is not available in the literature. Instead, the rate of reaction 15 was estimated based on a typical *A* factor (on a per H atom basis) and intrinsic activation energy from several $RH + O_2 \rightarrow R^\bullet + HO_2$ abstraction reactions.[25,45,46] This yielded an intrinsic activation energy of about 1 kcal/mol and an *A* factor of 1.2×10^{13} cm^3/(mol s) per H atom; including the endothermicity of reaction 15 gives $k_{15} \approx 3.6 \times 10^{13} \exp(-6900\ \text{K}/T)$ cm^3/(mol s). For the conditions of 1155 K and $\Phi = 0.89$ in Table I

$$k_{15}[O_2] \approx 17000\ \text{s}^{-1}$$

This value can be compared to the rate of competing reactions such as reaction 3 and 4

$$p\text{-}CH_3C_6H_4\dot{C}H_2 + O \rightarrow p\text{-}CH_3C_6H_4CHO + H \qquad (3)$$

$$p\text{-}CH_3C_6H_4\dot{C}H_2 + HO_2 \rightarrow p\text{-}CH_3C_6H_4CH_2O^\bullet + OH \qquad (4)$$

$$p\text{-}CH_3C_6H_4CH_2O^\bullet \rightarrow p\text{-}CH_3C_6H_4CHO + H$$

where the rates were estimated by collision theory[3] to be $k_3 \approx 1.6 \times 10^{13}$ cm^3/(mol s) and $k_4 \approx 3.2 \times 10^{12}$ cm^3/(mol s). Based on more recent work,[8,9] k_3 may be as high as 4×10^{14} cm^3/(mol s). A previous estimate of the O atom and HO_2 mole fractions,[11,20] showed that O atom and HO_2 reached concentrations of approximately 1×10^{-13} and 1×10^{-12} mol/cm^3, respectively. Using $k_3 = 4 \times 10^{14}$ cm^3/(mol s) for both k_3 and k_4 yields an upper limit of

$$k_3[O] + k_4[HO_2] \approx 400\ \text{s}^{-1}$$

which is over 40 times slower than $k_{15}[O_2]$ estimated earlier. Even by the approximate nature of the foregoing analysis, it is clearly evident that if the estimated rate for reaction 15 were correct, only *p*-xylylene would have been formed. This conclusion is certainly not supported by the experimental results where the presence of the sequential oxidation route, discussed in section IA, indicated a large contribution from reactions 3 and 4. Thus, the transition state for reaction 15 must be intermediate between the biradical and the methylenic state causing the intrinsic activation energy to be larger than that estimated above.

Based on the recent work of Slagle and co-workers on ethyl and O_2,[47,48] an alternative mechanism for reaction 2 might be possible. These investigators have shown that up to 1000 K the formation of the olefin from ethyl proceeds through an addition adduct followed by elimination of HO_2:

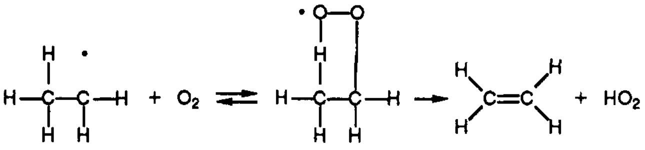

Because of delocalization of the odd electron about the aromatic ring,[49] an analogous reaction might be possible for methylbenzyl radical yielding the reaction scheme shown in Figure 14. Such an analogy is difficult to make though because (1) ESR spectra[49] have indicated that the delocalization effect is small (i.e., the electron density is highest at the CH_2 site), (2) the methylbenzyl reaction has an additional energy barrier associated with the overall endothermicity of 12.7 kcal/mol which is absent in the exothermic ethyl reaction, and (3) the scheme proposed by Slagle and co-workers has been studied below 1000 K and hence the role of direct abstraction at the temperatures studied here is unclear; certainly the addition adduct is less stable at higher temperatures making the adduct–elimination channel less important as the temperature increases. Thus, from these considerations, the preferred reaction mechanism for reaction 2 is direct abstraction of H by O_2.

---

(44) Mulcahy, M. F. R.; Williams, D. J. *Aust. J. Chem.* **1965**, *18*, 20.

(45) Norton, T. S.; Dryer, F. L. *Combust. Sci. Technol.* **1989**, *63*, 107.

(46) Yetter, R. A.; Dryer, F. L.; Rabitz, H. *Combust. Sci. Technol.*, to be published.

(47) Slagle, I. R.; Feng, Q.; Gutman, D. *J. Phys. Chem.* **1984**, *88*, 3648.

(48) Wagner, A. F.; Slagle, I. R.; Sarzynski, D.; Gutman, D. *J. Phys. Chem.* **1990**, *94*, 1853.

(49) Fleming, I. *Frontier Orbitals and Organic Chemical Reactions*; Wiley: London, 1976.